Sulfane Decreases the Nucleophilic Reactivity of Zinc Thiolates: Implications for Biological Reactive Sulfur Species

W.T. Michael Seo, Moises Ballesteros II, and Emily Y. Tsui*

Department of Chemistry and Biochemistry, University of Notre Dame, Notre Dame, IN, 46556, United States

ABSTRACT: A zinc dithiolate complex supported by a $[N_3S_2]$ ligand was studied as a model for zinc-mediated thiolate-disulfide exchange, enabling isolation of a zinc-bound mixed-disulfide intermediate. Solution-phase characterization of this zinc-disulfide complex indicates an interaction between the zinc center and the disulfide moiety that results in activation of the S-S bond for subsequent reactions. Comparison of this reaction with disulfide exchange by a previously prepared zinc tetrasulfanido complex demonstrates that sulfane sulfur (S^0) acts as an efficient thiolate trapping agent, i.e. polysulfanide anions are much less basic than thiolates. The resulting polysulfanide anions also exhibit decreased nucleophilicity compared to the parent thiolate anions. Alkylation kinetics comparisons between the zinc dithiolate and zinc tetrasulfanido complexes indicate attenuation of zinc-bound thiolate nucleophilicity by sulfane. These results suggest a general interplay between zinc, sulfane, and thiol/thiolate reactivity that can significantly impact biological redox processes.

INTRODUCTION

Sulfur-dependent reactions are critical components of biological redox signaling pathways related to disease and function in cardiovascular, immune, and other physiological systems.¹⁻² While H₂S has long been known to be a gasotransmitter, recent efforts have also pointed to the role of sulfur in the S⁰ oxidation state (sulfane), which participates via the intermediacy of hydropersulfides and other higher-order polysulfur compounds (Figure 1A).³⁻⁴ Metal centers in biology also commonly contribute to these signaling processes, for example in H₂S or hydrosulfide oxidation,⁵⁻⁷ polysulfide binding and redox,⁸ and mediation of protein persulfidation.⁹

Sulfane has been proposed to modulate the reactivity and other chemical properties (e.g. redox potentials, electrophilicity, and nucleophilicity) of biological thiol compounds.4 In particular, sulfur nucleophiles containing S-S bonds (e.g. perthiols) have been proposed to exhibit higher nucleophilicities than the corresponding parent thiols due to the α -effect,^{3, 10} the empirical observation that nucleophilic donors with adjacent lone-pair-containing heteroatoms exhibit increased nucleophilicity, in many cases. 11-12 However, direct measurement of these species is challenging due to complexities in polysulfide speciation; for example, thiolates in solution with added S₈ form dynamic mixtures of anionic organic polysulfanide species.¹³ This difficulty in isolating well-defined polysulfur-containing compounds has therefore limited experimental demonstration of the $\alpha\text{-effect}$ in these polysulfur compounds, whether in their protonated or free anionic forms. 14-16

Due to the ubiquity of zinc in biological contexts, much synthetic effort has gone into modeling zinc thiolate active sites, with particular attention to the impact of zinc on thiolate nucleophilicity in the context of thiolate alkylation or phosphoester cleavage. 17-21 Synthetic zinc complexes have also been shown to participate in both sulfane and disulfide activation. $^{22-24}$ Importantly, well-defined zinc polysulfanido (L_nZnS_xR , x=2, 4, R= alkyl or aryl) are isolable and have been structurally characterized, $^{25-26}$ making them useful potential precursors for studies of sulfane effects on thiolate nucleophilicity.

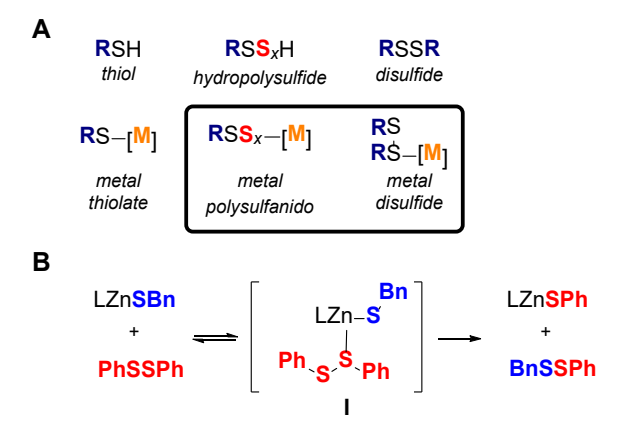


Figure 1. (A) Sulfur-containing compounds relevant to biological reactive sulfur species. (B) Zinc-mediated thiolate/disulfide exchange (L = tris(5-methyl-3-phenylpyrazolyl)borate).

In related chemistry, the reaction of thiols with disulfides, also known as thiol-disulfide exchange, is a central reaction in essential biological pathways such as signaling and redox homeostasis.27-28 The mechanism of this reaction has been extensively studied; for example, the kinetics of thiol-disulfide exchange have also been shown to be strongly affected by the surrounding environment (e.g. solvent)29-31 and thiol substituent.³⁰⁻³⁴ Biological zinc thiolates (e.g. in the thioredoxin family of metalloenzymes) are known to participate in a related thiolate-disulfide exchange reaction,³⁵ and the zinc ion has also been proposed to modulate the redox equilibrium between cellular thiols and disulfides. 36-37 However, the mechanistic details of this process have been less studied, although experimental and computational studies have suggested that zinc can accelerate thiol-disulfide exchange compared to the free thiols.³⁸⁻⁴⁰ In synthetic contexts, studies of pseudo-tetrahedral zinc thiolate/disulfide exchange have implicated the formation of intermediates in which disulfide compounds associate with the zinc thiolate moiety prior to S-S and Zn-S bond scrambling (I, Fig. 1B).38 However, such intermediates have not yet been isolated or otherwise characterized, and greater mechanistic understanding of the role of Zn^{2+} in these reactions is necessary.

Here, we report a study of sulfane effects on zinc thiolate reactivity with organic disulfide compounds. We isolate an unusual zinc-disulfide complex that is a proposed intermediate in zinc-mediated thiolate/disulfide exchange reactions and characterize the solution-phase intramolecular interactions between the disulfide bond with Zn²+. Further, we compare the nucleophilicities of well-defined zinc thiolate complexes and zinc tetrasulfanido complexes toward both alkylation and disulfide addition, demonstrating that the polysulfanido motif is, in our system, less nucleophilic than the thiolate analogue (i.e. no α -effect). The implications of these results on biological reactive sulfur species and their reactions (both mediated by zinc and not) are discussed.

RESULTS AND ANALYSIS

Identification of a Zinc-Disulfide Intermediate. Our group has reported a zinc dithiolate complex [1]²⁻ supported by a bis(carboxamide)pyridine framework that demonstrated the unusual insertion of elemental sulfur into the zinc-thiolate bond to form the zinc tetrasulfanido complex [2]²⁻ quantitatively (Scheme 1).²⁶ The oxidative rearrangement of [1]²⁻ forms a bimetallic complex [3]²⁻ containing a disulfide moiety that is not associated with a metal center.²⁶ We hypothesized that these complexes could be used to probe the relative nucle-ophilicities and basicities of zinc thiolate and zinc polysulfanido complexes.

Scheme 1. Sulfur Insertion and Oxidation of a Zinc Dithiolate Complex

We first investigated the reaction between organic disulfide compounds and $[1]^{2-}$ or $[2]^{2-}$. In DMSO- d_6 , dibenzyl disulfide and di-n-butyl disulfide do not scramble at room temperature over a period of several days. Addition of [Et₄N]₂[1] (10 mol %) to a 1:1 mixture of dibenzyl disulfide and di-n-butyl disulfide in DMSO- d_6 formed a statistical distribution of the homodisulfides and the mixed disulfide within minutes at room temperature. In comparison, the addition of [Et₄N]₂[2] (10 mol %) in DMSOd₆ to the same 1:1 dibenzyl disulfide/di-n-butyl disulfide mixture reaches the expected statistical distribution of homo- and mixed disulfide compounds over 2 h at room temperature. Over longer periods, sulfur was transferred to the disulfide compounds to form alkyl polysulfides and [1]2-. The discrepancy in disulfide scrambling rates indicates that the nucleophilic Zn-S moieties of [1]2- and [2]2- must exhibit very different nucleophilicities and/or thermodynamic stabilities relative to the alkyl disulfides and also to the free alkylthiolate anions.

In the above zinc-mediated disulfide exchange, the initial step of nucleophilic attack by the zinc-bound thiolate upon the organic disulfide compound should form an intermediate complex with a disulfide-containing ligand. Similar species have previously been proposed in zinc thiolate/disulfide exchange reactions, but have not been observed or characterized.³⁸ The

chelating bis(carboxamide)pyridine ligand framework in complexes [1]²⁻ and [2]²⁻ was expected to favor the formation of such a zinc-disulfide intermediate. Scheme 2 shows the formation of a proposed zinc-disulfide complex ($[4^{Me}]$ -) from the addition of $(p\text{-tolS})_2$ (p-tol = 4-methylphenyl) to $[1]^{2-}$. In this reaction, an equivalent of free thiolate anion [Et₄N][p-tolS] should also be formed as the byproduct. However, neither the proposed intermediate species nor the free thiolate anion was observed by ¹H NMR spectroscopy upon the addition of excess (p-tolS)₂ (10 equiv) to [1]²⁻, suggesting that the formation equilibrium constants of this intermediate is small. Similarly, treatment of DMSO- d_6 solutions of [1]²⁻ with other 4-substituted aryl disulfide compounds $[(4-R'C_6H_4S)_2, R' = NMe_2, NH_2, MeO,$ Me, H, Cl, CF_3] or with alkyl disulfide compounds (RSSR, R = Bu, Bn,, allyl) does not form any observable quantities of the corresponding expected zinc-disulfide complexes ([4R']- for aryl disulfides or $[5^R]$ for alkyl disulfides) or the free thiolate anion.

Scheme 2. Formation of a Zinc-Disulfide Intermediate ($[4^{\text{Me}}]^{-}$)

$$(\rho-\text{tol}\mathbf{S})_2$$

$$(p-\text{tol}\mathbf{S})_2$$

$$(p-\text{tol}\mathbf{S})_2$$

$$(p-\text{tol}\mathbf{S})_2$$

$$(p-\text{tol}\mathbf{S})_3$$

$$(p-\text{tol}\mathbf{S})_4$$

$$(p-\text{tol}\mathbf{S})_6$$

$$(p-\text{tol}\mathbf{S})_6$$

$$(p-\text{tol}\mathbf{S})_6$$

$$(p-\text{tol}\mathbf{S})_6$$

Lewis acids were used to sequester the thiolate anion by-product and to favor the formation of this proposed zinc-disulfide intermediate. Addition of BPh₃ or B(C_6F_5)₃ to a 1:1 mixture of [1]²⁻ and (p-tolS)₂ in DMSO- d_6 formed a new set of ¹H NMR signals, assigned as the disulfide-containing zinc complex [4^{Me}]²⁻ (Scheme 2). Stoichiometric ratios of [1]²⁻, (p-tolS)₂, and B(C_6F_5)₃ resulted in ca. 16% conversion of [1]²⁻ to [4^{Me}]⁻, and the maximum observed conversion to [4^{Me}]⁻ using excess disulfide (10 equiv) and B(C_6F_5)₃ (5 equiv) was 63% by ¹H NMR spectroscopy. The ¹⁹F NMR spectrum of [4^{Me}]⁻ prepared from the mixture of B(C_6F_5)₃, [1]²⁻, and (p-tolS)₂ also shows a new set of signals assigned as the borate anion [p-tolSB(C_6F_5)₃]^{-,41}

Similarly, addition of $(p\text{-tolS})_2$ (2.5 equiv) and CS₂ (50 equiv) to $[\mathbf{1}]^{2-}$ in DMSO- d_6 formed a mixture of $[\mathbf{4}^{\mathrm{Me}}]^-$ and $[\mathbf{1}]^{2-}$ in a 2.5:1 ratio, along with concomitant formation of p-tolyltrithio-carbonate (Fig. S35). A new $^1\mathrm{H}$ NMR signal at 2.30 ppm assigned to the $p\text{-CH}_3$ protons of the trithiocarbonate product is also present in a 1:1 ratio with $[\mathbf{4}^{\mathrm{Me}}]^-$. With 10 equiv $(p\text{-tolS})_2$ and 100 equiv CS₂, only the ligand-derived peaks corresponding to $[\mathbf{4}^{\mathrm{Me}}]^-$ are present by $^1\mathrm{H}$ NMR spectroscopy and $[\mathbf{1}]^{2-}$ can no longer be observed.

Complex $[4^{\text{Me}}]^-$ was independently prepared by sulfenylation of $[1]^{2-}$. Oxidative chlorination of 4-methylbenzenethiol by N-chlorosuccinimide followed by addition of the resulting p-tolSCl (1 equiv) to $[1]^{2-}$ in CH_3CN yielded a bright yellow solid. ^1H NMR spectroscopy of a DMSO- d_6 solution of this product reveals that $[4^{\text{Me}}]^-$ is the major product (Fig. S31). Additional ^1H NMR peaks corresponding to the bimetallic complex $[3]^{2-}$ and to $(p\text{-tolS})_2$ are also observed. Attempts at purification always resulted in a mixture of $[4^{\text{Me}}]^-$, $[3]^{2-}$ and $(p\text{-tolS})_2$, suggesting that the three species undergo dynamic exchange in solution (Eqn. 1), with a corresponding equilibrium constant K_{eq} as shown in Equation 2.

$$0.5 [3]^{2-} + 0.5 (p-R'C_6H_4S)_2 \rightleftharpoons [4^{R'}]^{-}$$
 (1)

$$K_{eq} = \frac{[[\mathbf{4}^{\mathbf{R}'}]^{-}]}{[[\mathbf{3}]^{2-}]^{0.5}[(p-\mathbf{R}'\mathbf{C}_{6}\mathbf{H}_{4})_{2}]^{0.5}}$$
(2)

A 1:1 mixture of [3]²⁻ and (p-tolS)₂ in DMSO- d_6 was monitored by ${}^1\mathrm{H}$ NMR spectroscopy. Signals corresponding to complex [4^{Me}]- increase over several days, finally reaching an equilibrium ratio of 4.4:1 [4^{Me}]- to [3]²⁻. Figure 2A compares the ${}^1\mathrm{H}$ NMR spectrum of a mixture of [4^{Me}]-, [3]²⁻ and (p-tolS)₂ prepared in this way to those of the [3]²⁻ and (p-tolS)₂ precursors. The same mixture with the addition of catalytic amounts of [1]²⁻ or of an organic thiolate anion such as [Et₄N][4-ClC₆H₄S] (<5 mol %) reached equilibrium within 24 h at room temperature, with K_{eq} = 4.44.

The formation of $[4^{Me}]$ - from $[3]^{2-}$ shown in Eqn. 1 occurs only by exchange of aryl disulfide S–S bonds. As such, this reaction would not be expected to strongly favor either direction based only on enthalpic reasons. While we cannot rule out other energetic contributions (e.g. strain or entropy), the observation that the formation of $[4^{R'}]$ - from $[3]^{2-}$ and substituted aryl disulfides have relatively high formation equilibrium constants suggests the possibility of an intramolecular interaction between the Zn^{2+} center and the organic disulfide moiety in $[4^{R'}]$ - that stabilizes this complex compared to $[3]^{2-}$, in which there is no interaction between the organic disulfide moiety of the ligand and the Zn^{2+} centers of the complex.

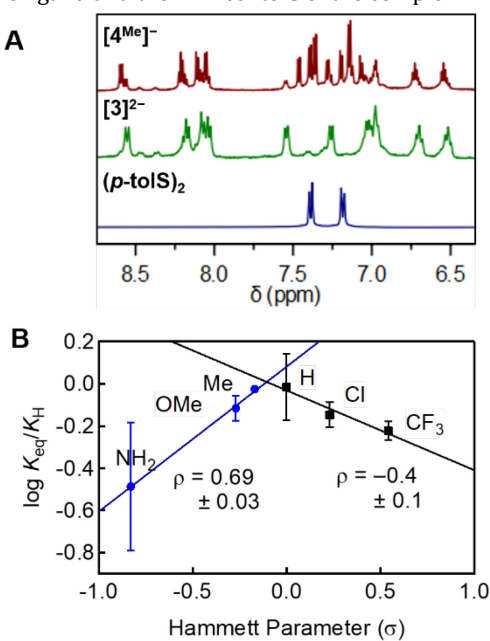


Figure 2. (A) ¹H NMR spectra of DMSO- d_6 solutions of [**4**^{Me}]-prepared from a mixture of [**3**]²⁻ and 1 equiv (p-tolS)₂ at 50° C for 3 d (red), [**3**]²⁻ (green), and (p-tolS)₂ (blue). (B) The ratio of $K_{\rm eq}/K_{\rm H}$ plotted vs. the Hammett parameter (σ) for the formation of [**4**^{R'}]-from the addition of p-substituted aryl disulfide compounds to [**3**]²⁻.

The equilibrium constants $K_{\rm eq}$ for formation of $[{\bf 4}^{\rm R'}]^-$ were measured for different p-substituted aryl disulfides (p-R'C₆H₄S)₂. Figure 2B plots $\log(K_{\rm eq}/K_{\rm H})$ against the Hammett parameter (σ), where $K_{\rm H}$ is the $K_{\rm eq}$ for R' = H in the exchange reaction between $[{\bf 3}]^{2-}$, $[{\bf 4}^{\rm R'}]^-$, and $({\bf 4}\text{-R'}C_6H_4S)_2$, i.e. a Hammett plot. Interestingly, a linear free energy relationship is not observed; instead, a somewhat V-shaped plot is observed, with ρ = +0.69 ± 0.03 for electron-donating substituents and ρ = -0.4

 \pm 0.1 for electron-withdrawing substituents, where ρ is the slope of the fitted lines. arise from polarization of the S–S bond in $[4^R]^-$. We note that $|\rho|<1$, indicating that the equilibrium of formation is not very sensitive to the aryl substituent of these disulfide complexes. However, one possible interpretation of this apparent shallow V-shape is that greater polarization of the S–S bond results in apparent destabilization of $[4^R]^-$ compared to $[3]^{2-}$, and that a more stabilizing intramolecular Zn-disulfide interaction occurs with unpolarized S–S bonds. In support of this argument, the p-position Hammett parameters (σ) of amide $(\sigma=0.00)$ or acetamide $(\sigma=-0.15)$ substituents⁴² are similar to those of H $(\sigma=0.00)$ and Me $(\sigma=-0.17)$, meaning that the disulfide bond of $[4^R]^-$ is least polarized when R'=H or Me.

Structural and Spectroscopic Characterization of the Zinc-Disulfide Intermediate. Isolation and structural characterization of $[4^R]$ - synthesized using neutral diaryl disulfides proved difficult due to dynamic exchange with $[3]^{2-}$, as described above. We therefore employed the dicationic disulfide bis(4-trimethylammoniophenyl) disulfide iodide ([4-Me₃NC₆H₄S]₂[I]₂) to afford the zwitterionic zinc-disulfide complex 4^{NMe_3} , which readily precipitated from a 1:1 mixture of $[3]^{2-}$ and $[p\text{-NMe}_3\text{-C}_6\text{H}_4\text{S}]_2[I]_2$ in acetonitrile (Fig. 3). The ¹H NMR spectrum of 4^{NMe_3} in DMSO- d_6 matches well with other $[4^R]$ - complexes (Fig. S24), but does not exchange with $[3]^{2-}$ due to the removal of the Et₄N+ counterions.

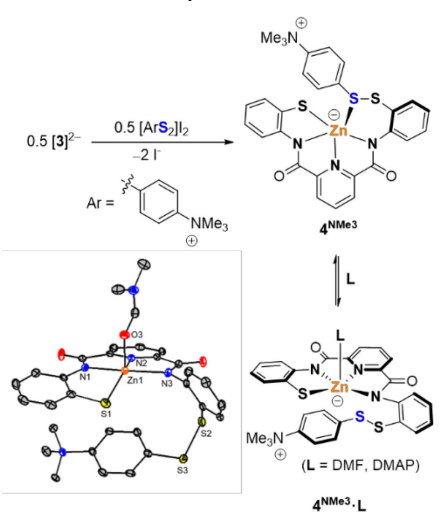


Figure 3. Synthesis of a zwitterionic zinc-disulfide complex (**4**NMe³) and solid-state structure of **4**NMe³·DMF (bottom left). Hydrogen atoms omitted for clarity.

Figure 3 shows the single-crystal X-ray diffraction (XRD) structure of crystals grown from vapor diffusion of methanol into a solution of 4^{NMe3} in N,N-dimethylformamide (DMF). This structure shows the expected product of disulfide exchange, but with a solvent DMF molecule bound through the oxygen atom to the zinc center in a distorted square pyramidal geometry (4^{NMe3} ·DMF). The geometric parameter τ was calculated to be 0.170 and the S—S [2.0402(9) Å] bond distance is typical of organic disulfides.43 The Zn—S bond distance of 2.2933(7) Å is slightly shorter than the median of those in previously published four-coordinate (2.34 Å) and five-coordinate (2.388 Å) zinc thiolate complexes. A similar structure of the related 0bound DMSO adduct (4NMe3.DMSO) was observed for crystals formed by layering a DMSO solution of 4NMe3 over trifluorotoluene (Fig. S53). Figure 3 shows the proposed formation of 4NMe3·L, in which the DMF or other Lewis basic molecule displaces the coordinated sulfur atom from the disulfide moiety of 4^{NMe3} .

Despite these solid-state data, there is evidence for solutionphase interactions between the pendant disulfide moiety and the zinc centers of complexes [4R']-. Firstly, a 1H NMR spectrum of a DMSO- d_6 solution of 4^{NMe3} with added DMF (5 equiv) shows broadening of the ligand-derived peaks, indicating exchange of multiple species (Fig. S28). These data do not rule out the possibility of simple conversion of 4NMe3.DMSO to 4NMe3. DMF, but addition of the stronger Lewis base 4-dimethylaminopyridine (DMAP, 2 equiv) to 4^{NMe3} in DMSO- d_6 resulted in upfield shifts in the resonances corresponding to the protons of the aryl ring situated between the disulfide and one of the ligand carboxamide moieties. This shift therefore indicates a significant comformational change, consistent with the solution-phase formation of 4NMe3. DMAP from 4NMe3. The comparatively more downfield resonances of 4NMe3 also support a Zndisulfide coordination in solution, in which the aryl protons are closer to the rest of the complex.

Secondly, compounds $[4^{R'}]$ are definitively monometallic in solution. The DOSY analysis of $[4^{Me}]$ - formed from $[1]^{2-}$, (ptolS)₂ (10 equiv), and CS₂ (100 equiv) in DMSO- d_6 measured the diffusion coefficient of $[4^{Me}]$ - to be 1.94×10^{-6} m²/s, close in value to those of [1]²⁻ (2.04 × 10⁻⁶ m²/s) and [2]²⁻ (1.87 × 10⁻⁶ m^2/s) but larger than that of the bimetallic complex [3]²⁻ (1.31) × 10⁻⁶ m²/s).²⁶ Based on the diffusion coefficient, a Stokes-Einstein-Gierer-Wirtz analysis⁴⁴⁻⁴⁵ estimates the formula weight of [4^{Me}] to be 541 g/mol; the theoretical formula weight for the structure as we have assigned it is 566 g/mol. While the reliability of this estimation is complicated by the charge of the complex, as the solvent shell is not accounted for, it supports our assignment of [4Me] - as a monometallic zinc-disulfide complex. Additionally, negative ion mode ESI-MS of independently prepared [4^{Cl}] - showed a signal at 583.9496 m/z, consistent with the theoretical value of 583.9301 m/z for [M]-.

While these results could be consistent with solvento species [4R']-DMSO with no disulfide-zinc interactions, we note that methylation of a thiolate moiety of [1]2-with MeI forms the corresponding thioether that undergoes rearrangement to form a bimetallic complex ([6Me]2-, Fig. 4).26 Similar bimetallic structures are formed upon alkylation with EtI, EtBr, or BnBr, and the solid-state structure of [6Bn]2- is also shown in Figure 4. This bimetallic structure likely forms because the thioether moiety is not a strong enough donor to zinc, and the resulting tetradentate, monoanionic ligand has a propensity for rearrangement and dimerization. As we can consider the ligand of $[6^{Bn}]^{2-}$ to be analogous to that of complex $[4^{H}]^{-}$, but with a methylene substituted for a disulfide sulfur atom, the observation that complexes [4R']- do not rearrange to form bimetallic structures may indicate an additional energetic factor that stabilizes the monometallic structure in $[4^R]$ - and $[5^R]$ -, which could be the Zn-S(disulfide) interaction.

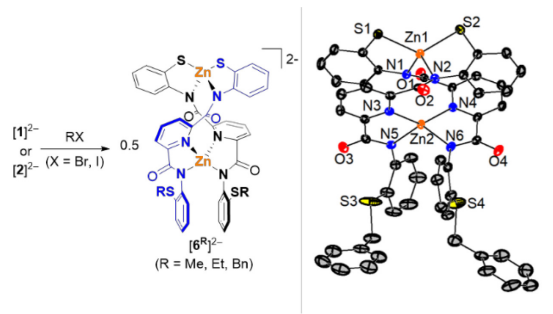


Figure 4. Alkylation of $[1]^{2-}$ or of $[2]^{2-}$ with alkyl halides forms bimetallic dithioether complexes ($[6^R]^{2-}$, left). Solid-state structure of $[6^{Bn}]^{2-}$ as 50% thermal ellipsoids (right). Hydrogen atoms and $[Et_4N]^+$ cations not shown for clarity.

Thirdly, Figure 5 compares the ATR-IR of solid-state samples of [3]²⁻, 4^{NMe3} prepared in the absence of coordinating Lewis bases, and crystalline 4NMe3. DMF. The IR spectrum of 4NMe3 displays a v_{S-S} band at 472 cm⁻¹, similar to that of a previously reported zinc-disulfide complex ($v_{S-S} = 490 \text{ cm}^{-1}$).⁴⁶ This vibrational mode occurs at a lower frequency than that of the bis(4trimethylammoniophenyl) disulfide precursor ($v_{S-S} = 481 \text{ cm}^{-1}$ 1)⁴⁷ and that of [3]²⁻ ($v_{S-S} = 480 \text{ cm}^{-1}$). The IR spectrum of crystals of 4NMe3·DMF show multiple weak bands between 470–480 cm⁻¹, consistent with displacement of disulfide from the zinc center by coordinated DMF. The vs-s band of 4NMe3 also occurs at lower energies compared to other zinc complexes containing S-S bonds that do not interact with the Zn²⁺ center, such as $[2]^{2-}$ ($v_{S-S} = 533$ cm⁻¹, Raman spectroscopy, Fig. S39). We also note that no Raman or IR vibration is observed near that of a previously reported and structurally related cobalt(III)-disulfide complex (509 cm⁻¹).⁴⁸ These results point to a an intramolecular interaction between Zn2+ and the disulfide moiety that weakens the S-S bond, as well as an electronic difference between Zn2+ and other transition metals that have been shown to exhibit metal-disulfide interactions.

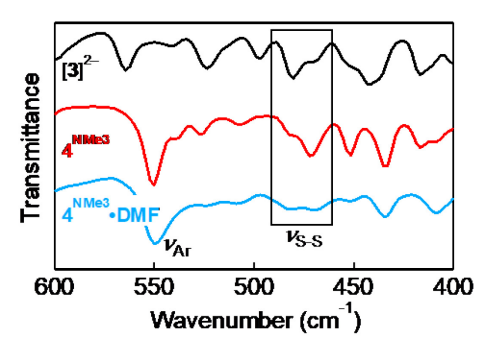


Figure 5. ATR-IR spectra of [3]^{2–}, 4^{NMe3} , and 4^{NMe3} -**DMF**. Bands assigned as v_{S-S} stretching modes are indicated. Spectra are scaled and offset for clarity.

Computational Studies of the Zinc-Disulfide Intermediate. To further understand the proposed zinc-disulfide interaction, we carried out geometry optimization and electronic structure calculations on the simplified variant $[5^{Me}]^-$ using DFT (B3LYP/def2tzvp). Figure 6 shows the optimized structure of this anionic species in DMSO, showing a S–Zn interaction of ca. 2.7 Å. This distance is similar to a previous structural characterized Zn-disulfide complex in which the ligand contained a pre-formed disulfide moiety (2.734(2) Å).

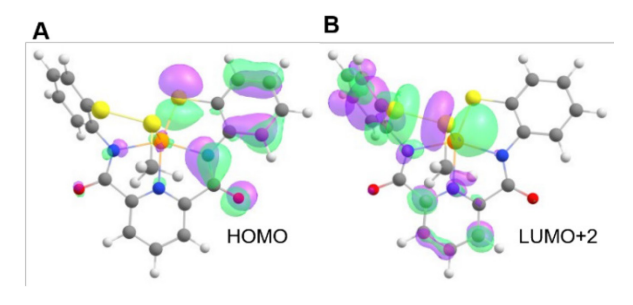


Figure 6. DFT calculated structure of [5^{Me}] - with (A) HOMO and (B) LUMO+2 molecular orbitals shown.

Figure 6 also shows the calculated HOMO and low-lying unoccupied orbitals. In these visualizations, the HOMO exhibits large contributions from the sulfur lone pair on the thiolate arm. Similarly, the low-lying unoccupied MOs (LUMO+1 and LUMO+2) show significant S–S σ^* character. Lower-lying occupied orbitals show the interaction between the disulfide moiety and the zinc center (Fig. S54), showing that these orbitals are available toward further nucleophilic attack in thiolate/disulfide exchange. The S–S stretching frequency was also calculated by DFT and found to be ca. 480 cm $^{-1}$, supporting our assignment of the vibrational spectrum of 4^{NMe3} .

From the above experimental and computational studies, the zinc-disulfide compounds $[4^R']$ - and $[5^R]$ - are unusual examples of complexes with a solution-phase interaction of the S atoms of a disulfide moiety with a Zn^{2+} center. A Cambridge Structural Database search of this connectivity reveals that although this type of interaction has been extensively demonstrated in the solid state with the first row transition metals Mn, Fe, Co, Ni, and Cu, $^{48-54}$ there is only one previously reported example with $Zn^{2+.46}$ Nevertheless, such zinc-disulfide species have been proposed as intermediates in previous examples of zinc-mediated disulfide/thiol exchange or disulfide reduction³⁹ and are also likely relevant in biological contexts (e.g. in zinc finger proteins and thiol-disulfide oxidoreductases). $^{55-57}$ Our results confirm the formation of these intermediates and suggest a role in disulfide coordination to zinc in further reactions.

Sulfane Drives Zinc-Disulfide Equilibria. To probe the effect of sulfane on the reactivity of Zn-S moieties and to compare the nucleophilicities of zinc thiolate and zinc polysulfanido motifs, we next studied the reaction between the welldefined zinc tetrasulfanido complex [2]2- and organic disulfides. The attack of the tetrasulfanido moiety on the aryl disulfide would be expected to form a diaryl pentasulfide complex, but such a species is not observed. Instead, the ¹H NMR spectrum of a DMSO- d_6 solution of $[2]^{2-}$ and diphenyl disulfide (PhSSPh, 1 equiv) shows the formation of $[4^{H}]^{-}$ in an approximately 1:1 ratio with [2]2- (Fig. S41). The ¹H NMR signals of [4H]- and [2]²⁻ coalesce at higher temperatures, demonstrating that this exchange is dynamic and reversible (Fig. S38). Figure 7A shows the absorption spectrum of a DMSO solution of [2]2and PhSSPh (5 equiv). Subtraction of the absorbance corresponding to [2]²⁻ shows the formation of a band at 495 nm (ε $\sim 590 \text{ M}^{-1} \text{ cm}^{-1}$), assigned to the phenylpolysulfanide anion (PhSS_x-) and consistent with previously characterized examples of phenyldisulfanide and phenylpolysulfanide anions.58 The intensity of this band increases with higher equivalents of PhSSPh (Fig. 7A inset, 0-3 equiv PhSSPh). The absorption spectrum of a mixture of S₈ and [Et₄N][4-ClC₆H₄S] in DMSO displays a similar feature (Fig. S46).

Scheme 3 shows the overall balanced reaction based on these data, in which the addition of a diaryl disulfide compound $(p-R'C_6H_4S)_2$ to $[\mathbf{2}]^{2-}$ forms $[\mathbf{4}^{R'}]^-$ and the corresponding free arylpolysulfanide anion, which is formed by addition of the free aryl thiolate anion to the three sulfur atom equivalents originating from $[\mathbf{2}]^{2-}$. This exchange is solvent-dependent; no signals corresponding to $[\mathbf{4}^{R'}]^-$ are observed in CD₃CN even with large excess of aryl disulfides. This is consistent with previous reports of solvent dependence in the solution equilibria of phenylpolysulfanide anions.⁵⁸

Scheme 3. Addition of Aryl Disulfides to $[2]^{2-}$ Forms $[4^{R'}]^-$

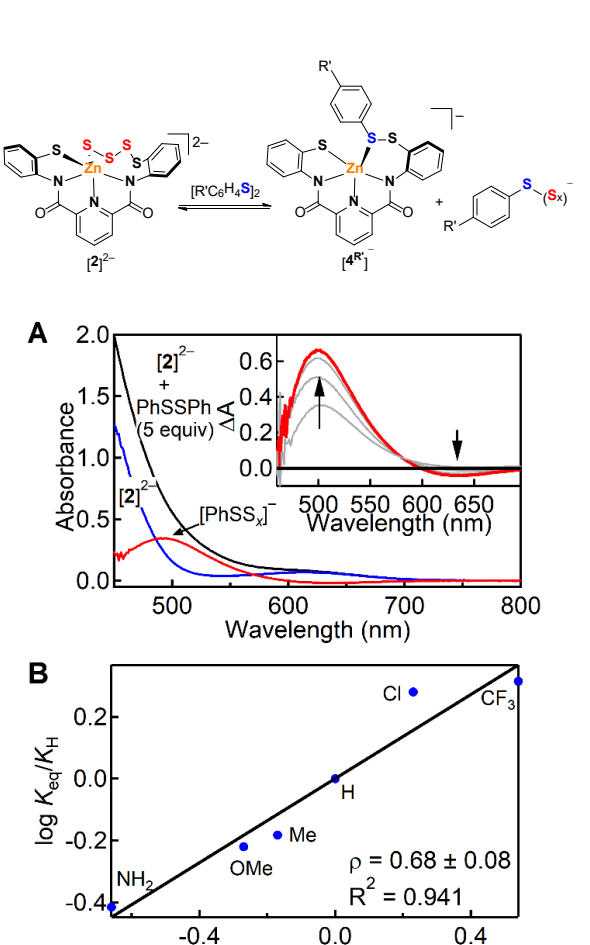


Figure 7. (A) Absorption spectra of a DMSO solution of $[Et_4N]_2[2]$ upon addition of diphenyl disulfide (0–5 equiv). Inset: Differential absorption of the above spectra. (B) Hammett plot of equilibrium constants of formation for $[4^R]$ - formed from $[2]^{2-}$ and $(p-R'C_6H_4S)_2$ plotted against the Hammett parameter (σ) of the *para* substituent.

Hammett Parameter (σ)

As described above, a 1:1 mixture of dithiolate complex [1]2and PhSSPh shows no detectable [4H]- by NMR spectroscopy, while a 1:1 mixture of [2]2- and PhSSPh results in 50% conversion of $[2]^{2-}$ to $[4^{H}]^{-}$. The addition of different p-substituted aryl disulfide compounds to [2]2- was studied by 1H NMR spectroscopy. Higher equilibrium constants of formation of [4R']were calculated for more electron-withdrawing *p*-substituents (Fig. S41). Figure 7B plots these equilibrium constants vs. the Hammett parameter of the *para* substituent. This plot displays a positive slope of ρ = +0.68, consistent with stabilization of negative charge by more electron-withdrawing substituents. The energy of this band also shifts with more electron-withdrawing substituents on the p-substituted aryl disulfide, as expected (Fig. S47). The intensity of the absorption band corresponding to the arylpolysulfanide anion in acetonitrile solution is approximately five times weaker than in DMSO, also consistent with a lower formation equilibrium constant in less polar solvents (Fig. S45).

The results above indicate that sulfane acts to perturb the equilibria as a "thiolate-trapping" Lewis acid, similar to the triarylboranes or to CS₂. Scheme 4 shows the relevant equilibria for the formation of the zinc-disulfide complexes $[4^R]^-$ and $[5^R]^-$ from $[1]^{2-}$ and $[2]^{2-}$ and organic disulfide compounds. From our data, the formation constant from $[1]^{2-}$, K_1 , is close to 0, meaning that $\Delta G_1 > 0$. In contrast, the formation constant

from [2]²⁻, K_2 , is larger (0 < K_2 < 2), meaning that ΔG_2 < ΔG_1 . Subtraction of these two equilibrium expressions therefore yields an equilibrium exchange between [1]²⁻, the "ArS₄-" anion, [2]²⁻, and the free aryl thiolate anion, which is expected to exhibit a more positive ΔG_3 .

Scheme 4. Relevant Equilibria for the Formation of $[4^{R'}]^-$ from $[1]^{2-}$ and $[2]^{2-}$, Respectively

$$\begin{bmatrix}
\mathbf{1}_{1}^{2} + \text{ArSSAr} & \frac{K_{1}}{\Longrightarrow} \begin{bmatrix}_{\mathbf{4}^{R'}_{1}} + \text{ArS} & \Delta G_{1} > 0 \\
\mathbf{2}_{1}^{2} + \text{ArSSAr} & \frac{K_{2}}{\Longrightarrow} \begin{bmatrix}_{\mathbf{4}^{R'}_{1}} + \text{"ArS}_{4}^{-"} & \Delta G_{2} < \Delta G_{1} \\
\mathbf{1}_{1}^{2} + \text{"ArS}_{4}^{-"} & \frac{K_{3}}{\Longrightarrow} \begin{bmatrix}_{\mathbf{2}_{1}^{2}} + \text{ArS} & \Delta G_{3} > 0
\end{bmatrix} = \Delta G_{1}^{2} + \Delta G_{2}^{2}$$

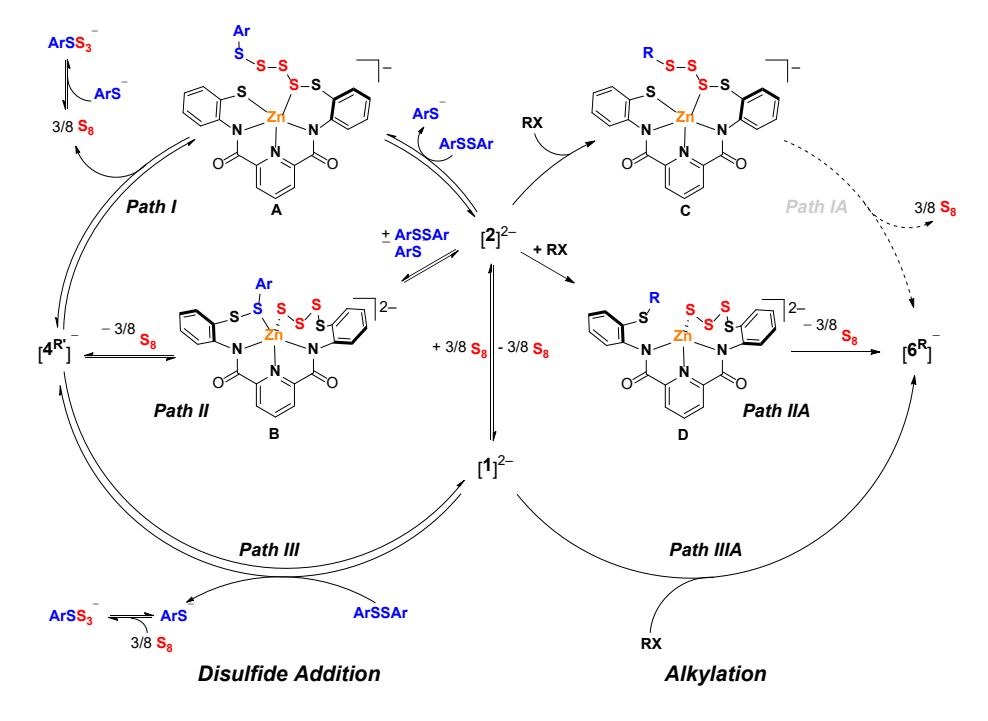
Previous computational and experimental studies have estimated that the Brønsted acidity of organic perthiols (RSSH) to be higher than that of organic thiols (RSH), with p K_a s lower by as much as 4 units, meaning that the RSS- anion is less basic than the corresponding thiolate anion (RS-).14-15 The equilibrium above ($K_3 \ll 1$) is consistent with sulfane-mediated decreased basicity of the free aryl thiolate anion. Additionally, the calculation that $\Delta G_3 > 0$, along with the assumption that the "RS₄H" species may also exhibit a lower pK_a than RSH, show that the corresponding zinc thiolate [1]2- is not correspondingly more basic than the tetrasulfanido [2]2-. This difference may arise from higher covalency between zinc and sulfur, meaning that Zn2+ behaves very differently from H+. We note that there are few examples of isolated metal polysulfanido complexes to permit a more general comparison of metal thiolate and metal polysulfanido basicities. We also note that the "tetrasulfanide anion" ArS₄- in the above equations is likely a distribution of thiolate and polysulfanide anions, as previously described (Eq. 3).58 As such, there may be a large, undetected entropic contribution that drives the reaction toward [1]2-. Regardless of the precise energetic components, however, it is clear that sulfane plays a role in changing the thermodynamic equilibria of these thiol/thiolate systems.

$$ArS^- + 3/8 S_8 \rightleftharpoons ArS_{2^-} + \frac{1}{4} S_8 \rightleftharpoons ArS_{3^-} + \frac{1}{8} S_8 \rightleftharpoons ArS_{4^-} (3)$$

Sulfane Effects on Zinc Thiolate Nucleophilicity. In addition to the above thermodynamic/basicity effects, we also probed the effects of sulfane on the kinetics/nucleophilicities of both organic thiolate anions and in the zinc tetrasulfanido moiety, as well as the mechanism of the unexpected formation of $[4^{R'}]$ - from [2]-. Scheme 5 shows possible routes to this species: in Path I, the tetrasulfanido moiety of [2]2- could add to the disulfide to form a pentasulfide compound (A) that then extrudes elemental sulfur to form [4^R]-. Alternatively (Path II), the zinc thiolate moiety of [2]2- could add to the disulfide to form a zinc-disulfide/tetrasulfanido intermediate (B) that then eliminates sulfur to form [4^R]-. As a third possibility (Path III), $[2]^{2-}$ could first lose sulfur to form $[1]^{2-}$, which then adds to the diaryl disulfide compound to form [4R']-. In this scenario, the free aryl thiolate anion then adds to sulfane to form a polysulfanide anion.

The kinetics of the formation of the zinc-disulfide complexes $[4^{R'}]$ and $[5^{R}]$ were measured. The addition of either $[1]^{2-}$ or $[2]^{2-}$ to diaryl disulfides to form $[4^{R}]^{-}$ is very fast, and we were unable to measure the rates of these reactions even at -50 °C in DMF. Treatment of [2]2- with BuSSBu to form [5Bu]- proceeded more slowly and could be monitored by ¹H NMR spectroscopy at room temperature. Figure 8 plots the concentrations of each zinc-containing species over time for a DMSO- d_6 solution of [2]²⁻ (14.2 mM) after treatment with BuSSBu (40 equiv), as measured by ¹H NMR spectroscopy. In these data, the formation of [5^{Bu}] and decay of [2]² do not follow single exponential functions, and are accompanied by the formation of [1]²- as well as by sulfur transfer to BuSSBu to form dibutyl polysulfide compounds (BuSS_xSBu, x > 0). These products could be formed by attack of butyl polysulfanide anions upon BuSSBu, or by attack of BuS- on putative intermediate A. As such, the proposed mechanism for this reaction requires multiple competing steps, several of which are not zinc-mediated, and does not permit us to distinguish the possible mechanistic pathways.

Scheme 5. Possible Pathways for Observed Products of Disulfide Addition or Alkylation of [2]2-



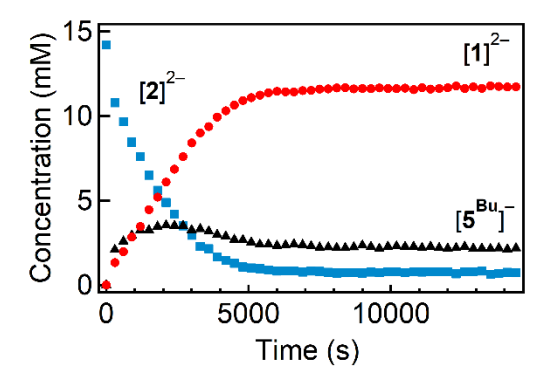


Figure 8. Concentrations of zinc-containing complexes measured by 1 H NMR spectroscopy after addition of BuSSBu (40 equiv) to a DMSO- d_6 solution of [2] $^{2-}$ (14.2 mM).

As a simpler reaction variant, the nucleophilicities of $[1]^{2}$ and $[2]^{2}$ were compared by studying the rates of ethylation of the respective Zn–S moieties upon addition of EtBr or EtI. The bimetallic ethylated complex $[6^{\rm Et}]^{2}$ was cleanly formed upon treatment of a DMSO- d_6 solution of $[1]^{2}$ with EtI (1 equiv) or EtBr (1 equiv) and displayed a similar 1 H NMR spectrum as that of $[6^{\rm Me}]^{2}$ (Fig. S32), as expected. The analogous treatment of a DMSO- d_6 solution of $[2]^{2}$ with one equivalent of EtI or EtBr formed multiple products, but the primary component of these mixtures (ca. 70%, 1 H NMR spectroscopy) was also the complex $[6^{\rm Et}]^{2}$, with little evidence of ethylpolysulfide species.

Although nucleophilic alkylation is different from nucleophilic addition to disulfides, the observation that complexes [1]²⁻ and [2]²⁻ again form the same final products suggest that the mechanism of [2]2- alkylation may be analogous to that of disulfide addition (Scheme 5, Path IA, IIA, or IIIA). The major difference in these steps, however, is that unlike S-S bonds, C-S bond formation should not be readily reversible. As such, this result suggests that alkylation of the tetrasulfanido moiety (Path IA, Scheme 5) is *not* the fastest step. Instead, $[6^R]^{2-}$ can only be formed by alkylation of the thiolate moiety of [2]2- or of [1]2- (Paths IIA and IIIA, Scheme 5). In either scenario, however, this product distribution indicates that zinc thiolate moieties are more nucleophilic than the zinc tetrasulfanido moiety by more than two-fold, given the ethylation product distribution. This result is also consistent with DFT calculations of the electronic structure of [2]²⁻, in which the HOMO exhibits large S(thiolate) *p*-orbital character, with smaller contributions from the tetrasulfanido S-centered orbitals (Fig. S55).

The electronic absorption spectra of a N,N-dimethylacetamide (DMA) solution of [$\mathbf{1}$]²⁻ (1.5 × 10⁻⁴ M) treated with EtBr (10 equiv) were monitored over 30 min at room temperature (Fig. S49). Spectral deconvolution of these data was used to calculate the concentration of [1]2- over time (Fig. 9). Additional experiments under pseudo-first-order conditions yield a rate constant for the second-order expression $k_1[[1^2-]][EtBr]$ of k_1 = $1.00 \pm 0.07 \text{ M}^{-1} \text{ s}^{-1}$. The electronic absorption spectra of a DMA solution of the zinc tetrasulfanido complex [2]²⁻ treated with EtBr were collected under identical conditions as described above. An approximate second-order rate constant k_2 = $0.28 \pm 0.07 \,\mathrm{M}^{-1}\,\mathrm{s}^{-1}$ for the ethylation of [2]²⁻ was estimated by spectral deconvolution (see SI). Figure 9 compares the concentrations of [1]2- and of [2]2- over time after treatment with EtBr. Altogether, the data presented here show that the rate of thiolate alkylation in [1]²⁻ is measurably faster than any of the possible alkylation pathways of [2]2-. We note that treatment

of $[\mathbf{6^{Et}}]^{2-}$ with a second equivalent of EtBr results in further alkylation of the remaining zinc thiolate moiety. However, the apparent rate of this second alkylation step was negligible in comparison to the first alkylation within the time window considered for the calculations.

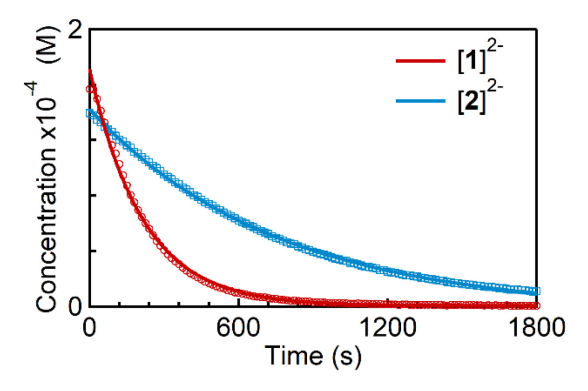


Figure 9. Concentrations of $[1]^{2-}$ or $[2]^{2-}$ over time after addition of EtBr (30 equiv) in DMA (1.5 × 10⁻⁴ M). Concentrations were determined by deconvolution of the absorption spectra.

In summary, these experiments show that alkylation of $[2]^{2}$ -proceeds by alkylation of a zinc thiolate moiety rather than the zinc tetrasulfanido moiety. We are unable to determine whether this reaction proceeds by thiolate alkylation of $[2]^{2}$ -(Path IIA) or alkylation of the small concentrations of $[1]^{2}$ - in equilibrium with $[2]^{2}$ - (Path IIIA), however, either step would be expected to be slower than that of only $[1]^{2}$ -. Regardless, we propose that the disulfide addition reactions proceed via similar thiolate addition steps (Paths II and III), rather than by tetrasulfanido addition (Path I).

DISCUSSION

Implications for the α -effect. The α -effect, as first described by Pearson, is the observation that nucleophiles containing a heteroatom with unshared electron pairs in the α -position exhibit higher nucleophilicities than expected purely from the nucleophile basicity. This effect has been experimentally demonstrated for N- or O-containing compounds like hydrazines, peroxides, and hydroxylamines (Fig. 10). Despite the well-established nature of this effect, its precise origin has been somewhat controversial; multiple explanations including transition state stabilization, ground state destabilization, and effects of HOMO orbital sizes or HOMO-LUMO gaps have been proposed. $^{59-62}$

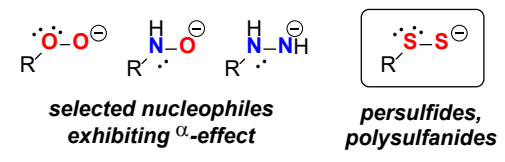


Figure 10. Motifs for the α -effect and compounds studied in this work.

The extension of this phenomenon to 3p elements such as sulfur is not as experimentally well-established. Sulfur is larger than oxygen and exhibits longer bond lengths and more diffuse p orbitals. 63 Due to these differences, a recent computational study on the α -effect has shown that nucleophiles such as MeSS- with S atoms in the α position show no α -effect, and in some cases, might even exhibit an "inverse α -effect." There are few experimental demonstrations of a sulfur α -effect. In organic solvents, a study of nitrobenzenethiolates with S_8 and

alkyl halides in DMA reported to observe a tenfold increase in reaction rate due to sulfane.16 In water, the acidity and nucleophilicity of glutathione persulfide was recently compared to that of glutathione. 15 Despite this comparatively sparser experimental evidence, this sulfur α-effect has been invoked in persulfide- or other sulfane-containing reactive sulfur species (RSS) that have recently been studied due to their importance in biological redox signaling.^{3, 10} Further experimental studies in this area are necessary, particularly as the relative nucleophilicities of sulfane-containing compounds has been demonstrated to greatly affect the outcomes of current methods used for quantification of reactive sulfur species in biological conditions.13 We note that the above discussion applies only to a twoelectron $\alpha\text{-effect}$; a one-electron $\alpha\text{-effect}$ is known, in which perthiyl radicals have been unambiguously demonstrated to be more stable than thiyl radicals.64

In our own studies of two-electron reactions, we were unable to directly measure the pK_a s of the zinc dithiolate complex $[1]^{2-}$ and the tetrasulfanido complex $[2]^{2-}$ due to competing protonolysis of the carboxamide ligand framework, and could not compare the nucleophilicity to the basicity.⁶⁰ Nevertheless, the alkylation studies described above definitively show that the tetrasulfanido moiety of $[2]^{2-}$ is far less nucleophilic toward alkylation than a zinc thiolate moiety, whether in $[1]^{2-}$ or in $[2]^{2-}$. This result contrasts with previously reported experimental comparisons of thiolate/perthiolate alkylation, in which the perthiolate exhibited orders of magnitude faster alkylation rate constants.¹⁵⁻¹⁶

These experimental discrepancies may point to a zinc-induced change in sulfur nucleophilicity. In our view, however, they instead arise from the difficulties in studying sulfane-containing RSS molecules due to the fast rate of sulfane exchange in these species, 13 and that the role of the zinc center in our studies serves to enable control over polysulfur nuclearity. In either case, these studies suggest that a sulfur α -effect should not necessarily be generally assumed to participate in the relative reactivities of RSS molecules under biological conditions, and that more work needs to be performed to understand how sulfane influences the reactivity of biological species.

CONCLUSIONS

We have presented a rare example of a zinc-bound, mixed-disulfide intermediate formed via disulfide interchange mediated by two zinc complexes supported by [N₃S₂] ligands, high-lighting the potential stabilizing and polarizing effects of Zn²⁺ on disulfide S–S bonds in solution. In addition, zinc thiolate moieties have been shown to be more nucleophilic than a zinc tetrasulfanido moiety. These findings serve as an example of sulfane attenuating, rather than enhancing, the nucleophilic reactivity of sulfur and suggest that the α -effect may not be as general a phenomenon for 3p elements like sulfur as is known for certain 2p elements, especially in the presence of biologically relevant metal centers such as Zn²⁺. Further studies in this area may provide insight into the interplay between transition metal ions and sulfane in both modulation of thiol/thiolate reactivity and sulfur transfer in biological and synthetic systems.

ASSOCIATED CONTENT

Supporting Information. Synthetic details, characterization data, including NMR and vibrational spectra, and methodology for kinetics experiments. This material is available free of charge via the Internet at http://pubs.acs.org.

AUTHOR INFORMATION

Corresponding Author

E-mail: etsui@nd.edu

ACKNOWLEDGMENT

This work was supported by NSF CHE-2047045 and by the University of Notre Dame. The authors thank Evgenii Kovrigin for assistance with NMR spectroscopy, Allen Oliver for assistance with X-ray crystallography, the Notre Dame Center for Research Computing, and Seth Brown for helpful discussions.

REFERENCES

- Wang, R. Physiological Implications of Hydrogen Sulfide: A Whiff Exploration That Blossomed. *Physiol. Rev.* 2012, 92, 791-896.
- Ida, T., Sawa, T., Ihara, H., Tsuchiya, Y., Watanabe, Y., Kumagai, Y., Suematsu, M., Motohashi, H., Fujii, S., Matsunaga, T., Yamamoto, M., Ono, K., Devarie-Baez, N. O., Xian, M., Fukuto, J. M., Akaike, T. Reactive Cysteine Persulfides and S-Polythiolation Regulate Oxidative Stress and Redox Signaling. *Proc. Natl. Acad. Sci. USA* 2014, 111, 7606-7611.
- Lau, N., Pluth, M. D. Reactive Sulfur Species (RSS): Persulfides, Polysulfides, Potential, and Problems. Curr. Opin. Chem. Biol. 2019, 49, 1-8.
- Filipovic, M. R., Zivanovic, J., Alvarez, B., Banerjee, R. Chemical Biology of H₂S Signaling through Persulfidation. *Chem. Rev.* 2018, 118, 1253-1337.
- Pluth, M. D., Tonzetich, Z. J. Hydrosulfide Complexes of the Transition Elements: Diverse Roles in Bioinorganic, Cluster, Coordination, and Organometallic Chemistry. *Chem. Soc. Rev.* 2020, 49, 4070-4134.
- Bostelaar, T., Vitvitsky, V., Kumutima, J., Lewis, B. E., Yadav, P. K., Brunold, T. C., Filipovic, M., Lehnert, N., Stemmler, T. L., Banerjee, R. Hydrogen Sulfide Oxidation by Myoglobin. *J. Am. Chem. Soc.* 2016, 138, 8476-8488.
- Vitvitsky, V., Yadav, P. K., An, S., Seravalli, J., Cho, U.-S., Banerjee, R. Structural and Mechanistic Insights into Hemoglobin-Catalyzed Hydrogen Sulfide Oxidation and the Fate of Polysulfide Products. *J. Biol. Chem.* 2017, 292, 5584-5592.
- Nelp, M. T., Zheng, V., Davis, K. M., Stiefel, K. J. E., Groves, J. T. Potent Activation of Indoleamine 2,3-Dioxygenase by Polysulfides. *J. Am. Chem. Soc.* 2019, 141, 15288-15300.
- Lange, M., Ok, K., Shimberg, G. D., Bursac, B., Markó, L., Ivanović-Burmazović, I., Michel, S. L. J., Filipovic, M. R. Direct Zinc Finger Protein Persulfidation by H₂S Is Facilitated by Zn²⁺. Angew. Chem. Int. Ed. 2019, 58, 7997-8001.
- Fukuto, J. M., Ignarro, L. J., Nagy, P., Wink, D. A., Kevil, C. G., Feelisch, M., Cortese-Krott, M. M., Bianco, C. L., Kumagai, Y., Hobbs, A. J., Lin, J., Ida, T., Akaike, T. Biological Hydropersulfides and Related Polysulfides – a New Concept and Perspective in Redox Biology. FEBS Lett. 2018, 592, 2140-2152.
- Jencks, W. P., Carriuolo, J. Reactivity of Nucleophilic Reagents toward Esters. J. Am. Chem. Soc. 1960, 82, 1778-1786.
- Edwards, J. O., Pearson, R. G. The Factors Determining Nucleophilic Reactivities. J. Am. Chem. Soc. 1962, 84, 16-24.
- Bogdándi, V., Ida, T., Sutton, T. R., Bianco, C., Ditrói, T., Koster, G., Henthorn, H. A., Minnion, M., Toscano, J. P., van der Vliet, A., Pluth, M. D., Feelisch, M., Fukuto, J. M., Akaike, T., Nagy, P. Speciation of Reactive Sulfur Species and Their Reactions with Alkylating Agents: Do We Have Any Clue About What Is Present inside the Cell? *Br. J. Pharmacol.* 2019, 176, 646-670.
- Cuevasanta, E., Lange, M., Bonanata, J., Coitiño, E. L., Ferrer-Sueta, G., Filipovic, M. R., Alvarez, B. Reaction of Hydrogen Sulfide with Disulfide and Sulfenic Acid to Form the Strongly Nucleophilic Persulfide. *J. Biol. Chem.* 2015, 290, 26866-26880.
- Benchoam, D., Semelak, J. A., Cuevasanta, E., Mastrogiovanni, M., Grassano, J. S., Ferrer-Sueta, G., Zeida, A., Trujillo, M., Möller, M. N., Estrin, D. A., Alvarez, B. Acidity and Nucleophilic Reactivity of Glutathione Persulfide. J. Biol. Chem. 2020, 295, 15466-15481.
- Benaïchouche, M., Bosser, G., Paris, J., Plichon, V. Relative Nucleophilicities of Aryldisulphide and Thiolate Ions in Dimethylacetamide Estimated from Their Reaction Rates with Alkyl Halides. J. Chem. Soc., Perkin 2 1990, 1421-1424.

- Wilker, J. J., Lippard, S. J. Modeling the DNA Methylphosphotriester Repair Site in Escherichia Coli Ada. Why Zinc and Four Cysteines? *J. Am. Chem. Soc.* 1995, 117, 8682-8683.
- Wilker, J. J., Lippard, S. J. Alkyl Transfer to Metal Thiolates: Kinetics, Active Species Identification, and Relevance to the DNA Methyl Phosphotriester Repair Center of Escherichia Coli Ada. *Inorg. Chem.* 1997, 36, 969-978.
- Smith, J. N., Shirin, Z., Carrano, C. J. Control of Thiolate Nucleophilicity and Specificity in Zinc Metalloproteins by Hydrogen Bonding: Lessons from Model Compound Studies. *J. Am. Chem. Soc.* 2003, 125, 868-869.
- Rombach, M., Seebacher, J., Ji, M., Zhang, G., He, G., Ibrahim, M. M., Benkmil, B., Vahrenkamp, H. Thiolate Alkylation in Tripod Zinc Complexes: A Comparative Kinetic Study. *Inorg. Chem.* 2006, 45, 4571-4575.
- Picot, D., Ohanessian, G., Frison, G. The Alkylation Mechanism of Zinc-Bound Thiolates Depends Upon the Zinc Ligands. *Inorg. Chem.* 2008, 47, 8167-8178.
- Sahana, T., Kakkarakkal, D. C., Kundu, S. Cross-Talks between Sulfane Sulfur and Thiol at a Zinc(II) Site. Chem. Eur. J. 2022, 28, e202200776.
- Naskar, T., Pal, N., Majumdar, A. Synthesis and Redox Reactions of Binuclear Zinc(II)-Thiolate Complexes with Elemental Sulfur. New J. Chem. 2021, 45, 22406-22416.
- Hossain, K., Majumdar, A. Polysulfido Chain in Binuclear Zinc(II) Complexes Br. Inorg. Chem. 2022, 61, 6295-6310.
- Galardon, E., Tomas, A., Selkti, M., Roussel, P., Artaud, I. Synthesis, Characterization, and Reactivity of Alkyldisulfanido Zinc Complexes. *Inorg. Chem.* 2009, 48, 5921-5927.
- Ballesteros, M., Tsui, E. Y. Reactivity of Zinc Thiolate Bonds: Oxidative Organopolysulfide Formation and S3 Insertion. *Inorg. Chem.* 2019, 58, 10501-10507.
- Barron, E. S. G. Thiol Groups of Biological Importance. In Advances in Enzymology and Related Areas of Molecular Biology, Wiley, 1951; pp 201-266.
- Namboodiri, M. A. A., Favilla, J. T., Klein, D. C. Pineal N-Acetyltransferase Is Inactivated by Disulfide-Containing Peptides: Insulin Is the Most Potent. Science 1981, 213, 571-573.
- Snyder, G. H., Cennerazzo, M. J., Karalis, A. J., Locey, D. Electrostatic Influence of Local Cysteine Environments on Disulfide Exchange Kinetics. *Biochemistry* 1981, 20, 6509-6519.
- Singh, R., Whitesides, G. M. Comparisons of Rate Constants for Thiolate-Disulfide Interchange in Water and in Polar Aprotic Solvents Using Dynamic Proton NMR Line Shape Analysis. J. Am. Chem. Soc. 1990, 112, 1190-1197.
- Fernandes, P. A., Ramos, M. J. Theoretical Insights into the Mechanism for Thiol/Disulfide Exchange. *Chem. Eur. J.* 2004, 10, 257-266.
- 32. Wilson, J. M., Bayer, R. J., Hupe, D. J. Structure-Reactivity Correlations for the Thiol-Disulfide Interchange Reaction. *J. Am. Chem. Soc.* **1977**, *99*, 7922-7926.
- Shaked, Z. e., Szajewski, R. P., Whitesides, G. M. Rates of Thiol-Disulfide Interchange Reactions Involving Proteins and Kinetic Measurements of Thiol pKa Values. *Biochemistry* 1980, 19, 4156-4166.
- Houk, J., Whitesides, G. M. Structure-Reactivity Relations for Thiol-Disulfide Interchange. J. Am. Chem. Soc. 1987, 109, 6825-6836.
- Maret, W. Oxidative Metal Release from Metallothionein Via Zinc-Thiol/Disulfide Interchange. Proc. Natl. Acad. Sci. USA 1994, 91, 237-241
- Jiang, L.-J., Maret, W., Vallee, B. L. The Glutathione Redox Couple Modulates Zinc Transfer from Metallothionein to Zinc-Depleted Sorbitol Dehydrogenase. Proc. Natl. Acad. Sci. USA 1998, 95, 3483-3488.
- Maret, W., Vallee, B. L. Thiolate Ligands in Metallothionein Confer Redox Activity on Zinc Clusters. *Proc. Natl. Acad. Sci. USA* 1998, 95, 3478-3482.
- Boerzel, H., Koeckert, M., Bu, W., Spingler, B., Lippard, S. J. Zinc-Bound Thiolate–Disulfide Exchange: A Strategy for Inhibiting Metallo-B-Lactamases. *Inorg. Chem.* 2003, 42, 1604-1615.
- Amirnasr, M., Bagheri, M., Farrokhpour, H., Schenk, K. J., Mereiter, K., Ford, P. C. New Zn(II) Complexes with N₂S₂ Schiff Base Ligands. Experimental and Theoretical Studies of the Role of Zn(II) in Disulfide Thiolate-Exchange. *Polyhedron* 2014, 71, 1-7.

- Kurian, R., Bruce, M. R. M., Bruce, A. E., Amar, F. G. The Influence of Zinc(II) on Thioredoxin/Glutathione Disulfide Exchange: Qm/Mm Studies to Explore How Zinc(II) Accelerates Exchange in Higher Dielectric Environments. *Metallomics* 2015, 7, 1265-1273.
- Dureen, M. A., Welch, G. C., Gilbert, T. M., Stephan, D. W. Heterolytic Cleavage of Disulfides by Frustrated Lewis Pairs. *Inorg. Chem.* 2009, 48, 9910-9917.
- Hansch, C., Leo, A., Taft, R. W. A Survey of Hammett Substituent Constants and Resonance and Field Parameters. *Chem. Rev.* 1991, 91, 165-195.
- Addison, A. W., Rao, T. N., Reedijk, J., van Rijn, J., Verschoor, G. C. Synthesis, Structure, and Spectroscopic Properties of Copper(II) Compounds Containing Nitrogen–Sulphur Donor Ligands; the Crystal and Molecular Structure of Aqua[1,7-Bis(N-Methylbenzimidazol-2'-Yl)-2,6-Dithiaheptane]Copper(II) Perchlorate. *J. Chem. Soc., Dalton Trans.* 1984, 1349-1356.
- Evans, R., Deng, Z., Rogerson, A. K., McLachlan, A. S., Richards, J. J., Nilsson, M., Morris, G. A. Quantitative Interpretation of Diffusion-Ordered NMR Spectra: Can We Rationalize Small Molecule Diffusion Coefficients? *Angew. Chem. Int. Ed.* 2013, 52, 3199-3202.
- Evans, R., Dal Poggetto, G., Nilsson, M., Morris, G. A. Improving the Interpretation of Small Molecule Diffusion Coefficients. *Anal. Chem.* 2018, 90, 3987-3994.
- 46. Bremer, J., Wegner, R., Krebs, B. Zur Konkurrenz Von Stickstoff-Und Schwefel-Donoratomen in Zinkkomplexen: [Zn(Bims)₂][SiF₆] · 5MeOH Und [ZnCl(Paps)]₂(Zn₂Cl₆) (Bims = Bis(2-Benzimidazolylmethyl)Sulfid; Paps = O,O ' -(N,N ' Dipicolinyliden)Diazadiphenyldisulfid). Z. Anorg. Allg. Chem. 1995, 621, 1123-1132.
- Chen, J.-X., Zhang, W.-H., Tang, X.-Y., Ren, Z.-G., Zhang, Y., Lang, J.-P. Assembly of a New Family of Mercury(II) Zwitterionic Thiolate Complexes from a Preformed Compound [Hg(Tab)₂](PF₆)₂ [Tab = 4-(Trimethylammonio)Benzenethiolate]. *Inorg. Chem.* 2006, 45, 2568-2580
- Nosco, D. L., Elder, R. C., Deutsch, E. A Rational Synthesis of Coordinated Disulfides from Coordinated Thiols. Crystal Structure of [(en)2Co(S(SC2H5)CH2CH2NH2)](ClO4)3.H2O. *Inorg. Chem.* 1980, 19, 2545-2551.
- Riley, P. E., Seff, K. Crystal and Molecular Structure of Chloro(Bis {2-[(2-Pyridylmethyl)Amino]Ethyl} Disulfide)Nickel(II) Perchlorate. *Inorg. Chem.* 1972, 11, 2993-2999.
- Bertrand, J. A., Breece, J. L. Preparation and Structure of Chloro(Bis{Salicylideniminephenyl}Disulfido)Iron(III). *Inorg. Chim. Acta* 1974, 8, 267-272.
- Warner, L. G., Kadooka, M. M., Seff, K. Structural Trans Effect at Nickel(II). Crystal and Molecular Structure of Bromo[Bis(2-((2-Pyridylmethyl)Amino)Ethyl) Disulfide]Nickel(II) Perchlorate. *Inorg. Chem.* 1975, 14, 1773-1778.
- Boorman, P. M., Kerr, K. A., Kydd, R. A., Moynihan, K. J., Valentine, K. A. Synthetic, Structural, and Spectroscopic Studies of the Ligating Properties of Organic Disulphides: X-Ray Structure of Copper(I) Iodide–Diethyl Disulphide. J. Chem. Soc., Dalton Trans. 1982, 1401-1405
- Lydon, J. D., Elder, R. C., Deutsch, E. Synthesis and Characterization of Coordinated Disulfides. Single-Crystal Structural Analysis of [(en)2Co(S(SC(CH3)2COOH)C(CH3)2COO)](ClO4)2.H2O. *Inorg. Chem.* 1982, 21, 3186-3197.
- Kessissoglou, D. P., Butler, W. M., Pecoraro, V. L. Characterization of Mono- and Binuclear Manganese(II) Schiff Base Complexes with Metal-Disulfide Ligation. *Inorg. Chem.* 1987, 26, 495-503.
- Barbirz, S., Jakob, U., Glocker, M. O. Mass Spectrometry Unravels Disulfide Bond Formation as the Mechanism That Activates a Molecular Chaperone. *J. Biol. Chem.* 2000, 275, 18759-18766.
- Tang, W., Wang, C.-c. Zinc Fingers and Thiol–Disulfide Oxidoreductase Activities of Chaperone Dnaj. *Biochemistry* 2001, 40, 14985-14994.
- Shi, Y.-y., Tang, W., Hao, S.-f., Wang, C.-C. Contributions of Cysteine Residues in Zn2 to Zinc Fingers and Thiol-Disulfide Oxidoreductase Activities of Chaperone Dnaj. *Biochemistry* 2005, 44, 1683-1689.
- 58. Jungen, S., Paenurk, E., Chen, P. Synthesis, Spectroscopic, and Structural Characterization of Organyl Disulfanides and a Tetrasulfanide. *Inorg. Chem.* **2020**, *59*, 12322-12336.

- Um, I.-H., Buncel, E. The Origin of the α-Effect: Dissection of Ground-State and Transition-State Contributions. J. Org. Chem. 2000, 65, 577-582.
- Um, I.-H., Im, L.-R., Buncel, E. Pitfalls in Assessing the α-Effect: Reactions of Substituted Phenyl Methanesulfonates with HOO-, OH-, and Substituted Phenoxides in H₂O. *J. Org. Chem.* 2010, 75, 8571-8577.
- Garver, J. M., Gronert, S., Bierbaum, V. M. Experimental Validation of the α-Effect in the Gas Phase. *J. Am. Chem. Soc.* 2011, 133, 13894-13897.
- 62. Hansen, T., Vermeeren, P., Bickelhaupt, F. M., Hamlin, T. A. Origin of the α -Effect in S_N2 Reactions. *Angew. Chem. Int. Ed.* **2021**, 60, 20840-20848.
- 63. 15 Sulfur. In *Chemistry of the Elements (Second Edition)*, Greenwood, N. N.; Earnshaw, A., Eds. Butterworth-Heinemann: Oxford, 1997; pp 645-746.
- Chauvin, J.-P. R., Griesser, M., Pratt, D. A. Hydropersulfides: H-Atom Transfer Agents Par Excellence. J. Am. Chem. Soc. 2017, 139, 6484-6493

